

Assignment of individual heme EPR signals of *Desulfovibrio baculatus* (strain 9974) tetraheme cytochrome c_3

A redox equilibria study

Isabel MOURA¹, Miguel TEIXEIRA¹, Boi H. HUYNH², Jean LeGALL³ and José J. G. MOURA¹

¹ Centro de Química Estrutural, Complexo I, UNL, Lisboa

² Department of Physics, Emory University, Atlanta, GA

³ Department of Biochemistry, University of Georgia, Athens, GA

(Received March 7/May 25, 1988) – EJB 88 0294

An EPR redox titration was performed on the tetraheme cytochrome c_3 isolated from *Desulfovibrio baculatus* (strain 9974), a sulfate-reducer. Using spectral differences at different poised redox states of the protein, it was possible to individualize the EPR g -values of each of the four hemes and also to determine the mid-point redox potentials of each individual heme: heme 4 (–70 mV) at $g_{\max} = 2.93$, $g_{\text{med}} = 2.26$ and $g_{\min} = 1.51$; heme 3 (–280 mV) at $g_{\max} = 3.41$; heme 2 (–300 mV) at $g_{\max} = 3.05$, $g_{\text{med}} = 2.24$ and $g_{\min} = 1.34$; and heme 1 (–355 mV) at $g_{\max} = 3.18$. A previously described multi-redox equilibria model used for the interpretation of NMR data of *D. gigas* cytochrome c_3 [Santos, H., Moura, J. J. G., Moura, I., LeGall, J. & Xavier, A. V. (1984) *Eur. J. Biochem.* 141, 283–296] is discussed in terms of the EPR results.

Low-potential tetraheme cytochromes c_3 (molecular mass circa 13 kDa) are found in sulfate-reducing bacteria belonging to the genus *Desulfovibrio* [1]. They have been indicated as playing a role in electron transfer linked to energy-yielding processes, namely hydrogen production/consumption via the hydrogenase enzyme, but at the present moment their physiological role is still controversial.

Each heme in this class of cytochromes is bound to the protein polypeptide chain by two thioether linkages involving cysteine residues and the fifth and sixth heme-iron ligands are histidyl residues.

Structural studies by X-ray crystallography have been reported for cytochrome c_3 isolated from *D. vulgaris* (strain Myazaki) [2] and *D. baculatus* (strain Norway 4) [3] (previously known as *D. desulfuricans* strain Norway 4). The four hemes are localized in non-equivalent protein environments and each heme has a negative and a different mid-point redox potential. The small size of the protein and the high number of heme groups present suggested the existence of heme-heme interactions. The cytochrome c_3 was described as a protein containing interacting redox centers by the NMR study of the redox equilibria in *D. vulgaris* (strain Hildenborough) and *D. gigas* cytochrome c_3 [4–6].

In principle, the non-equivalent four-redox-center molecule can have 16 redox states in a multi-redox electron distribution equilibria [5] (Fig. 1). Furthermore, the redox properties of each center may be affected by the redox states of the adjacent centers due to heme-heme interactions. Thus, a complete characterization of each individual center in such a complex system requires a large number of parameters and may be difficult to perform. However specialized spectroscopic techniques, namely NMR and EPR, have been used to probe each heme individually and to provide valuable information concerning the interplay between the redox centers. The proton-NMR spectra of the tetraheme cytochrome c_3

from *D. gigas* were examined while varying the pH and the redox potential [5]. The analysis of the NMR data was based on a model that takes into consideration all the redox species present in the solution and showed that heme-heme interac-

STATE 4 \rightleftharpoons STATE 3 \rightleftharpoons STATE 2 \rightleftharpoons STATE 1 \rightleftharpoons STATE 0

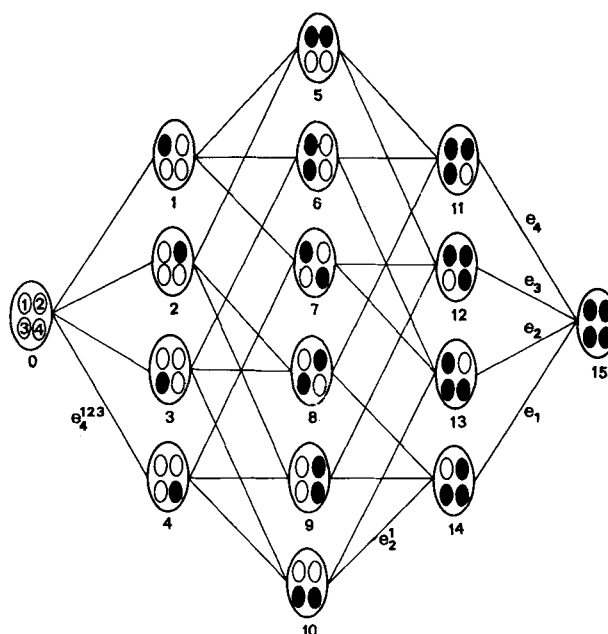


Fig. 1. Schematic representation of the multiredox equilibria in tetraheme cytochrome c_3 . Definition of the redox states and micro (e_i) redox potentials involved (adapted from [5]). Microscopic mid-point potentials (e_i , e_i^j , e_i^{jk} , e_i^{jkl} where $i, j, k, l = 1, 2, 3$ and 4, heme 1 being the most negative) can be defined by 32 Nernst equilibria between each pair of states. As an example, e_2^1 is defined as the mid-point potential of heme 2 when heme 1 is oxidized and hemes 3 and 4 (unspecified) are reduced

tions resulted in a change of redox properties in a range between -50 mV and $+60$ mV. The heme mid-point redox potentials as well as the interacting potentials were shown to be pH-dependent.

EPR potentiometric titrations have also been performed in tetraheme cytochromes c_3 [7–11]. Although the experimental data were poorly resolved in the low-field region (g_{\max}), tentative assignments have been made and the values of four mid-point redox potentials for the heme groups have been determined using four independent Nernst equations.

In a recent paper Gayda et al. [11] have shown that the redox potentials previously determined for the tetraheme cytochrome c_3 isolated from *D. baculatus* (strain Norway 4) [9] were not correctly determined due to a wrong attribution of the EPR signals. By accounting for the total intensity of the EPR spectra the four macroscopic redox potentials of the tetraheme cytochrome c_3 from *D. baculatus* (strain Norway 4) were determined to be -150 mV, -270 mV, -325 mV and -355 mV [11].

In this article we report an EPR redox titration on the cytochrome c_3 from *D. baculatus* (strain 9974). Using the method of differential spectroscopy, we were able to resolve and assign the four g_{\max} resonances to the four heme groups, and determine the four corresponding redox potentials with one being a true microscopic value.

MATERIALS AND METHODS

Cytochrome c_3 was isolated from *D. baculatus* (strain 9974) and purified as previously described [12].

Anaerobic oxidation-reduction titration of the cytochrome c_3 was carried out as detailed in [13]. The cytochrome c_3 solution ($830 \mu\text{M}$ in 0.1 M Tris/HCl at pH 8.1) was poised at different potentials in the presence of oxidation-reduction mediators, all at $10 \mu\text{M}$ and at 25°C . The mediators used were phenosafranine, benzylviologen, methylviologen and 2-hydroxy-(1,4)-naphthoquinone. The potential was adjusted by addition of small amounts of dithionite or ferricyanide solutions. After equilibration at a fixed potential, a sample was transferred into an EPR tube under argon and immediately frozen at 77K for posterior EPR quantification. All redox potentials are quoted versus a normal hydrogen electrode (NHE).

EPR spectra were recorded in a Bruker ER-200 tt equipped with an Aspect computer and an Oxford Instruments continuous-flow cryostat.

RESULTS AND DISCUSSION

In Fig. 2 we present the EPR spectra obtained for cytochrome c_3 from *D. baculatus* (strain 9974) poised at different redox potentials. The spectrum of the native cytochrome is similar to that previously published and described [9]. In the early stages of the redox titration, the intensity of the shoulder at $g \approx 2.9$ decreases with the lowering of the potential and is no longer observed at -201 mV.

The EPR spectrum of the heme with the highest redox potential (heme 4) can be easily obtained ($g_{\max} = 2.93$, $g_{\text{med}} = 2.26$, $g_{\min} = 1.51$; Fig. 3D) by taking the difference between the spectra of the native sample ($+200$ mV) and the sample at -157 mV.

By sequential differences using the oxidized spectrum ($+200$ mV) as reference, the intensity of the EPR signals due to heme 4 can be measured as a function of the redox potential.

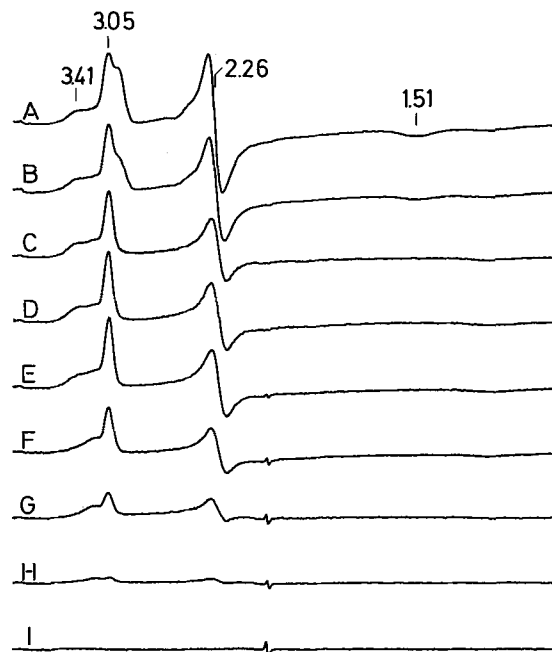


Fig. 2. EPR redox titration of *D. baculatus* (strain 9974) tetraheme cytochrome c_3 . Selected EPR spectra are shown for samples at the following poised redox potentials: (A) $+200$ mV, (B) -46 mV, (C) -91 mV, (D) -134 mV, (E) -201 mV, (F) -291 mV, (G) -320 mV, (H) -366 mV, (I) -466 mV. EPR experimental conditions: microwave power 0.1 mW, temperature 10 K, modulation amplitude 1.0 mT, sweep time 500 s, protein concentration $830 \mu\text{M}$.

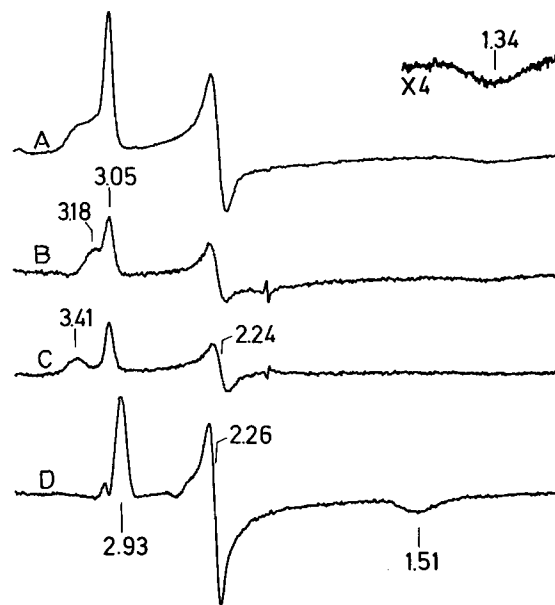


Fig. 3. EPR spectral differences obtained at chosen redox potentials in order to assign spectral components. Experimental data was obtained as indicated in Fig. 2. (A) EPR spectrum of *D. baculatus* cytochrome c_3 at -157 mV (not shown in Fig. 2). (B) Difference spectrum obtained from spectra of samples poised at -157 mV and the difference spectra obtained as indicated in C (this last component was multiplied by a factor 1.7). (C) Difference spectrum obtained from spectra of samples poised at -157 mV and at -291 mV (spectrum F, Fig. 2). (D) Difference spectra obtained from spectra of samples poised at $+200$ mV and at -157 mV.

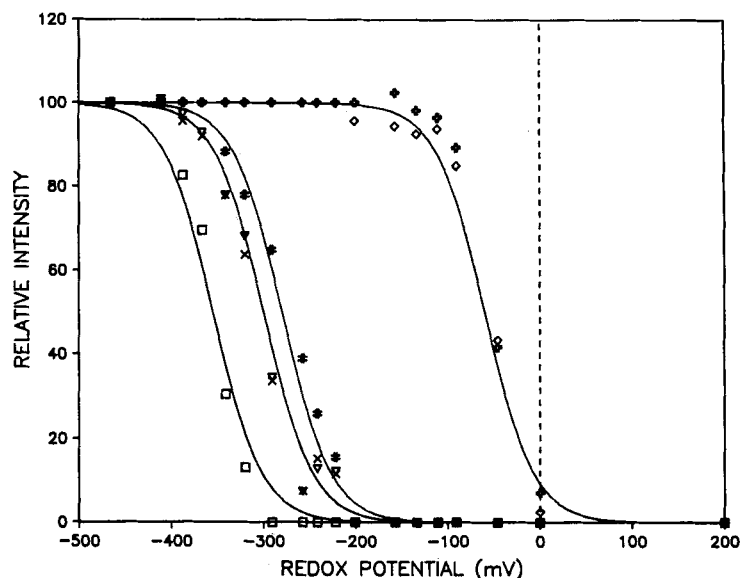


Fig. 4. EPR intensity of each individual component measured from the experimental redox data shown in Fig. 2 and manipulated by spectral differences as indicated in Fig. 3. Heme 4 (\diamond , $g_{\max} = 2.93$ and \square , $g_{\text{med}} = 2.26$); heme 3 ($\#$, $g_{\max} = 3.41$); heme 2 (\times , $g_{\max} = 3.05$ and ∇ , $g_{\text{med}} = 2.24$); heme 1 (\square , $g_{\max} = 3.18$). The theoretical curves were calculated from the model described in the text, without considering interacting potentials and using the following mid-point redox potential values -355 mV, -300 mV, -280 mV and -70 mV (equivalent to considering four independent Nernst equations with $n = 1$)

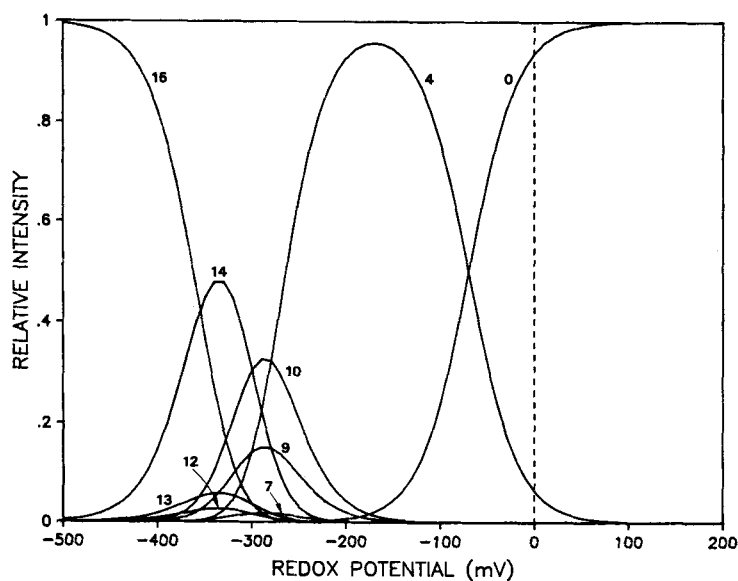


Fig. 5. Population distribution curves for the contributing oxidation states assuming a non-interacting model and four different mid-point redox potentials (see caption Fig. 4)

The spectrum obtained at -157 mV was then used as a new reference, since at this potential cytochrome c_3 only contains three oxidized hemes, hemes 3, 2 and 1 (Fig. 3A) and spectral differences enables us to follow the reduction of hemes 3 and 2. The g_{\max} value of heme 3 is clearly identified at 3.41 and heme 2 has $g_{\max} = 3.05$, $g_{\text{med}} = 2.24$ and $g_{\min} = 1.34$. The reduction of heme 1 ($g_z = 3.18$) can be followed by an identical method using the EPR spectrum of the sample at -291 mV as reference. Using the described procedure the intensity of the signals for each individual heme can be followed during the complete EPR redox titration.

In Fig. 4 the intensities of each heme are plotted against the poised solution redox potential.

Previously, we have successfully applied a model for the electron distribution in a tetraheme cytochrome [5]. In this

model, 16 redox species are assumed to be interconvertable during the oxidation-reduction process and four macroscopic reduction steps are considered which correspond to the successive entry of one electron (on going from fully oxidized to fully reduced states) (Fig. 1).

Using this model it is possible to calculate the 16 P_n populations as a function of the solution redox potential, E , if the absolute values of four microscopic redox potentials and six interacting potentials are known. The equations were fully developed in Appendix A of [5]. The use of these equations for the EPR data analysis can then be easily adapted. The alteration of the magnetic properties of the hemes upon reduction, going from a paramagnetic EPR-active state ($S = 1/2$) to a diamagnetic EPR-silent state ($S = 0$), implies that the spectral intensities observed (INT) must be the result of

the sum of populations of the species containing the oxidized hemes, which can be calculated as follows:

$$\text{INT (heme 4)} \\ = P_0 + P_1 + P_2 + P_3 + P_5 + P_6 + P_8 + P_{11}$$

$$\text{INT (heme 3)} \\ = P_0 + P_1 + P_2 + P_4 + P_5 + P_7 + P_9 + P_{12}$$

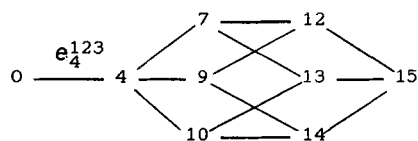
$$\text{INT (heme 2)} \\ = P_0 + P_1 + P_3 + P_4 + P_6 + P_7 + P_{10} + P_{13}$$

$$\text{INT (heme 1)} \\ = P_0 + P_2 + P_3 + P_4 + P_8 + P_9 + P_{10} + P_{14}$$

These intensities can then be computed using a simple computer program that takes into consideration the ten described parameters (four microscopic redox potential and six interacting potentials) and the experimental data are visually fitted with the theoretical curves.

A complete fitting of the experimental data can only be made by choosing a set of microscopic potentials (e_i^{kl}) and interacting potentials (I_{ij}) that can be adjusted to the experimental points. In the case under study, the three interacting potentials I_{24} , I_{34} and I_{14} cannot be estimated, since heme 4 has a very high and different mid-point redox potential and is completely reduced prior to the reduction of hemes 3, 2 and 1. The microscopic redox potential measured for heme 4 represents a value of e_4^{123} which by definition is the microscopic mid-point potential of heme 4 when hemes 3, 2 and 1 are oxidized.

A survey of the relative values of the fractional populations as a function of solution redox potential, using the estimated values for a non-interacting model (Fig. 5) indicates that redox species 1, 2, 3, 5, 6, 8 and 11 are negligible. The multi-redox equilibria between the different oxidation states can then be simplified and described schematically as follows:



and the equations used for computation of the EPR signal intensities can be simplified as:

$$\text{INT (heme 4)} \approx P_0$$

$$\text{INT (heme 3)} \approx P_0 + P_4 + P_7 + P_9 + P_{12}$$

$$\text{INT (heme 2)} \approx P_0 + P_4 + P_7 + P_{10} + P_{13}$$

$$\text{INT (heme 1)} \approx P_0 + P_4 + P_9 + P_{10} + P_{14}$$

In principle a curve-fitting program could be used in a convergent way in order to estimate the values of the interacting potentials that can best adjust to the experimental data from each set of values of e_1 , e_2 and e_3 previously imposed.

At the present moment however we refrain from presenting such an analysis, since the dispersion obtained with our experimental data can not give an unambiguous fitting. The experimental titration curves of each individual heme were then fitted with one-electron reduction theoretical curves deduced from a non-interacting model, using the following values: heme 1 (−355 mV), heme 2 (−300 mV), heme 3 (−280 mV) and heme 4 (−70 mV) (Fig. 4).

The mid-point redox potentials determined for *D. baculatus* (strain 9974) cytochrome c_3 reveal that one of the hemes has a very high and different value (−70 mV) com-

Table 1. Heme assignment in *D. baculatus* tetraheme cytochrome c_3 . The hemes of *D. baculatus* (strain 9974) are numbered according to their mid-point redox potential E_m measured versus a normal hydrogen electrode (this work). Hemes have been assigned according to X-ray structural data and EPR information alone (a), plus chemical modification [18] (b) and plus degree of exposure to solvent [3] (c)

Heme number	g_{\max}	E_m	Assignment of hemes according to		
			(a)	(b)	(c)
		mV			
1	3.18	−355	II or IV	II or IV	II or IV
2	3.05	−300	I or III	III	I
3	3.41	−280	IV or II	IV or II	IV or II
4	2.93	−70	III or I	I	III

pared with the other three. A high and well separated mid-point redox potential was also found for one of the hemes in *D. baculatus* (strain Norway 4) cytochrome c_3 (−150 mV) [11] and for the *Desulfobulbus elongatus* cytochrome c_3 (−30 mV) [14]. These observations, however, are not generally observed for this class of proteins. *D. vulgaris* (Myazaki) cytochrome c_3 has a narrow span of mid-point redox potential values (−230, −300, −310 and −360 mV) [10].

Another important result of the EPR analysis presented in this paper is the possibility of determining the g_{\max} value of the individual hemes. EPR, Mössbauer and structural studies of a series of well defined low-spin model compounds have provided conclusive evidence that the so-called 'strong- g_{\max} ' EPR signals (g_{\max} larger than 3.0) can be correlated with axial ligand symmetry and, in the case of planar axial ligands, a 'strong- g_{\max} ' signal represents a perpendicular alignment of the ligand planes [15–17]. In the cytochrome c_3 from *D. baculatus* (strain 9974) two hemes were identified to have g_{\max} values higher than 3.0 (heme 1 and heme 3), suggesting that the three-dimensional structure of this cytochrome should have two hemes where the histidyl ligands are not coplanar.

As has been pointed out, a close similarity exists between this cytochrome c_3 and that isolated from *D. baculatus* (strain Norway 4) [12]; they are the two proteins belonging to this homologous class of cytochromes for which close analogies are found [15]. Consequently it is reasonable to assume that their tertiary structures are also similar.

Using the available X-ray coordinates (Brookhaven Data Bank) for cytochrome c_3 from *D. baculatus* (Norway 4) and a Molecular Graphic Model (in collaboration with Drs J. Wampler and D. E. Stewart, Department of Biochemistry, University of Georgia at Atlanta), analysis of the histidyl heme ligands reveals that two of the hemes have their two axial ligands in a non-coplanar arrangement [3]. This analysis and the EPR results suggest a structural assignment for *D. baculatus* (strain 9974) hemes 1 and 3 to hemes II and IV, namely, they are the two hemes with non-coplanar ligand arrangement¹.

It was previously proposed by Haser et al. [3] that the heme with the highest redox potential should be heme III due to its lower degree of exposure to the solvent. This proposal does not agree with the heme assignment made by Dolla et al. which indicates that heme I has the highest redox potential

¹ The roman numbers presented in the text for numbering the hemes are the ones used in the X-ray structure description [3]. The cardinal numbers used in this article are in accordance with the redox potential, heme 4 having the highest redox potential heme, as already numbered in our previous paper [5].

value [18]. These authors chemically reacted the arginine residue 73 with cyclo-hexane-1,2-dione and studied the redox properties of the modified *D. baculatus* (Norway 4) cytochrome c_3 . Electrochemistry and molecular modeling indicated that heme I [3] (referred as heme 4 in [18], since in their paper hemes were numbered sequentially from the amino-terminus) was the closest to the single modified residue and corresponded to the heme group whose redox properties are the most affected after chemical modification. However, structural identity of both native and modified cytochromes remains to be demonstrated.

At the present moment we have no solid ground for a definitive assignment, as seen in Table 1 summarizing the results obtained, correlating the mid-point redox potential values with the EPR g -values (this work) and the X-ray structural assignments [3] and the chemical modification data [18]. Putting together the available information, the identification of heme I/heme III and heme II/heme IV, in correlation to mid-point redox potential and EPR g -values is still ambiguous.

This research was supported by grants from *Instituto Nacional de Investigação Científica*, *Junta Nacional de Investigação Científica e Tecnológica* and from NATO (to J.J.G.M.), the National Science Foundation (to J.LeG.) and National Institutes of Health (grant GM 32187 to B.H.H.). We thank Dr G. Fauque for valuable discussions.

REFERENCES

1. LeGall, J. & Fauque, G. (1988) in *Biology of anaerobic organisms* in *Environmental microbiology of anaerobes* (Zehnder, A. J. B., ed.) Chapter 11, in the press.
2. Higushi, Y., Kusanagi, M., Yasuoka, N., Kakuko, M. & Yagi, T. (1981) *J. Biochem. (Tokyo)* **90**, 1715–1723.
3. Haser, R., Pierrot, M., Frey, M., Payan, F., Astier, J. P., Bruschi, M. & LeGall, J. (1979) *Nature (Lond.)* **282**, 806–810.
4. Moura, J. J. G., Santos, H., Moura, I., LeGall, J., Moore, G. R., Williams, R. J. P. & Xavier, A. V. (1982) *Eur. J. Biochem.* **127**, 151–155.
5. Santos, H., Moura, J. J. G., Moura, I., LeGall, J. & Xavier, A. V. (1984) *Eur. J. Biochem.* **141**, 283–296.
6. Xavier, A. V. (1986) *J. Inorg. Chem.* **28**, 239–243.
7. DerVartanian, D. V., Xavier, A. V. & LeGall, J. (1978) *Biochimie (Paris)* **60**, 321–325.
8. Xavier, A. V., Moura, J. J. G., LeGall, J. & DerVartanian, D. V. (1979) *Biochimie (Paris)* **61**, 680–695.
9. Cammack, R., Fauque, G., Moura, J. J. G. & LeGall, J. (1984) *Biochim. Biophys. Acta* **784**, 68–74.
10. Gayda, J. P., Yagi, T., Bénosman, H. & Bertrand, P. (1987) *FEBS Lett.* **1**, 57–61.
11. Gayda, J. P., Bertrand, P., More, C., Guerlesquin, F. & Bruschi, M. (1985) *Biochim. Biophys. Acta* **829**, 262–267.
12. Fauque, G. (1985) *These de Doctorat d'Etat*, Université de Technologie, Compiègne.
13. Dutton, P. L. (1971) *Biochim. Biophys. Acta* **226**, 63–80.
14. Samin, E., Albagnac, G. & LeGall, J. (1986) *FEBS Lett.* **204**, 247–250.
15. Moura, I., Xavier, A. V., Moura, J. J. G., Fauque, G., LeGall, J. & Huynh, B. H. (1985) *Rev. Port. Quim.* **27**, 212–215.
16. Walker, F. A., Huynh, B. H., Scheidt, W. R. & Osvath, S. R. (1986) *J. Am. Chem. Soc.* **108**, 5288–5297.
17. Palmer, G. (1985) *Biochem. Soc. Trans.* **13**, 548–560.
18. Dolla, A., Cambillau, C., Bianco, P., Haladjian, J. & Bruschi, M. (1987) *Biochem. Biophys. Res. Commun.* **147**, 818–823.